19. Glöckner, G. *et al.* The complex repeats of *Dictyostelium discoideum*. *Genome Res.* **11,** 585–594 (2001).
20. Dear, P. H. in *Genome Mapping—A Practical Approach* (ed. Dear, P. H.) 95–124 (IRL Press, Oxford, 1997).
21. Pan, W. C. & Blackburn, E. H. Single extrachromosomal ribosomal RNA gene copies are synthesized during amplification of the rDNA in *Tetrahymena*. *Cell* **23,** 459–466 (1981).
22. Lim, L. P. & Burge, C. B. A computational analysis of sequence features involved in recognition of short introns. *Proc. Natl Acad. Sci. USA* **98,** 11193–11198 (2001).
23. Morio, T. *et al.* The *Dictyostelium* developmental cDNA project: generation and analysis of expressed sequence tags from the first-finger stage of development. *DNA Res.* **5,** 335–340 (1998).
24. Apweiler, R. *et al.* InterPro—an integrated documentation resource for protein families, domains and functional sites. *Bioinformatics* **16,** 1145–1150 (2000).
25. Goebl, M. G. & Petes, T. D. Most of the yeast genomic sequences are not essential for cell growth and division. *Cell* **46,** 983–992 (1986).
26. Konfortov, B. A., Cohen, H. M., Bankier, A. T. & Dear, P. H. A high-resolution HAPPY map of *Dictyostelium discoideum* chromosome 6. *Genome Res.* **10,** 1737–1742 (2000).
27. Lowe, T. M. & Eddy, S. R. tRNAscan-SE: a program for improved detection of transfer RNA genes in genomic sequence. *Nucleic Acids Res.* **25,** 955–964 (1997).
28. Parra, G., Blanco, E. & Guigo, R. GeneID in *Drosophila*. *Genome Res.* **10,** 511–515 (2000).
29. The Gene Ontology Consortium. Gene ontology: tool for the unification of biology. *Nature Genet.* **25,** 25–29 (2000).
30. Fortini, M. E., Skupski, M. P., Boguski, M. S. & Hariharan, I. K. A survey of human disease gene counterparts in the *Drosophila* genome. *J. Cell Biol.* **150,** F23–F30 (2000).

Supplementary Information accompanies the paper on *Nature*'s website (http://www.nature.com/nature).

Acknowledgements

We thank S. Förste, N. Zeisse, S. Rothe, S. Landmann, R. Schultz, S. Müller and R. Müller for expert technical assistance. We also thank the working team of the Japanese cDNA project (http://www.csm.biol.tsukuba.ac.jp/cDNAproject.html) for sharing data. The sequencing of chromosome 2 was supported by the Deutsche Forschungsgemeinschaft, with partial support by Köln Fortune. Additional support was obtained from the NIH, the Medical Research Council and the EU. Members of the Sanger Institute *Dictyostelium discoideum* sequencing team are listed at http://www.sanger.ac.uk/Projects/D_discoideum/team.shtml.

Competing interests statement

The authors declare that they have no competing financial interests.

Correspondence and requests for materials should be addressed to A.A.N. (e-mail: noegel@uni-koeln.de) or G.G. (e-mail: gernot@imb-jena.de).

|| The *Dictyostelium* Genome Sequencing Consortium (members not included in the main author list):

Sequencing and Analysis:
The Sanger Institute Dictyostelium sequencing team (led by Bart G. Barrell & Marie-Adèle Rajandream)[1], Jeffrey G. Williams[2], Robert R. Kay[3], Adam Kuspa[4], Richard Gibbs[4], Richard Sucgang[4], Donna Muzny[4] & Brian Desany[4]

Generation of cYAC library:
Kathy Zeng[5], Baoli Zhu[5] & Pieter de Jong[5]

Advisory Committee for the DFG-funded project:
Theodor Dingermann[6], Günther Gerisch[7], Peter Philippsen[8], Michael Schleicher[9], Stephan C. Schuster[10] & Thomas Winckler[6]

1, The Sanger Institute, Wellcome Trust Genome Campus, Hinxton, Cambridgeshire CB10 1SA, UK; 2, University of Dundee, MSI/WTB Complex, Dundee, UK; 3, MRC Laboratory, of Molecular Biology, Cambridge CB2 2QH, UK; 4, Baylor College of Medicine, Houston, Texas 77030, USA; 5, Children's Hospital Oakland – BACPAC Resources, Oakland, California 94609, USA; 6, Institut für Pharmazeutische Biologie, Universität Frankfurt (Biozentrum), Frankfurt am Main, 60439, Germany; 7, Max-Planck-Institut für Biochemie, 82152 Martinsried, Germany; 8, Molecular Microbiology, Biozentrum der Universität, 4056 Basel, Switzerland; 9, A.-Butenandt-Institut/Zellbiologie, Ludwig-Maximilians-Universität, 80336 München, Germany; 10, Max-Planck-Institut für Entwicklungsbiologie, 72076 Tübingen, Germany

Intracellular calcium stores regulate activity-dependent neuropeptide release from dendrites

Mike Ludwig*, Nancy Sabatier*, Philip M. Bull*, Rainer Landgraf†, Govindan Dayanithi‡ & Gareth Leng*

** Department of Biomedical Sciences, University of Edinburgh Medical School, George Square, Edinburgh EH8 9XD, UK*
† Max Planck Institute of Psychiatry, Clinical Institute, Kraepelinstraße 2-10, 80804 Munich, Germany
‡ Department of Neurobiology, INSERM 432, University of Montpellier II, Place Eugene Bataillon, F-34094 Montpellier, Cedex 5, France

Information in neurons flows from synapses, through the dendrites and cell body (soma), and, finally, along the axon as spikes of electrical activity that will ultimately release neurotransmitters from the nerve terminals. However, the dendrites of many neurons also have a secretory role, transmitting information back to afferent nerve terminals[1–4]. In some central nervous system neurons, spikes that originate at the soma can travel along dendrites as well as axons, and may thus elicit secretion from both compartments[1]. Here, we show that in hypothalamic oxytocin neurons, agents that mobilize intracellular Ca^{2+} induce oxytocin release from dendrites without increasing the electrical activity of the cell body, and without inducing secretion from the nerve terminals. Conversely, electrical activity in the cell bodies can cause the secretion of oxytocin from nerve terminals with little or no release from the dendrites. Finally, mobilization of intracellular Ca^{2+} can also prime the releasable pool of oxytocin in the dendrites. This priming action makes dendritic oxytocin available for release in response to subsequent spike activity. Priming persists for a prolonged period, changing the nature of interactions between oxytocin neurons and their neighbours.

Neurons in the supraoptic nucleus (SON) of the hypothalamus project axons to the posterior pituitary, where oxytocin and vasopressin are secreted from axonal nerve terminals into the systemic circulation. These peptides are also released in large amounts from dendrites in the SON[5], but secretion at these two sites is not consistently correlated. Suckling evokes oxytocin release in the SON[6] before significant peripheral secretion, whereas after osmotic stimulation, SON oxytocin release lags behind peripheral secretion[7]. During lactation, in response to suckling, oxytocin cells discharge with brief, intense bursts[8]; these bursts release boluses of oxytocin into the circulation that result in milk let-down from the mammary glands. The bursting activity can be blocked by central administration of oxytocin antagonists[9], thus central as well as peripheral oxytocin is essential for milk let-down. It has been proposed that suckling evokes dendritic oxytocin release that acts in a positive feedback manner to evoke bursting[10].

Oxytocin mobilizes intracellular Ca^{2+} from thapsigargin-sensitive stores in oxytocin cells[11]. Here we tested the hypothesis that this might be critical for dendritic oxytocin release. In anaesthetized rats, we implanted a microdialysis probe into the SON to measure oxytocin release in response to systemic osmotic stimulation. In some of these experiments we applied thapsigargin directly to the SON through the dialysis probe. Thapsigargin caused a significant increase in SON oxytocin release that returned to control levels after washout. Subsequent systemic osmotic stimulation (2 ml of 1.5 M NaCl, intraperitoneal injection) caused a much larger release of oxytocin in thapsigargin-pretreated rats than in controls. Osmotically stimulated oxytocin secretion into the circulation was unaffected by exposure of one SON to thapsigargin (Fig. 1a, b).

To test whether thapsigargin potentiated spike-dependent release

from the SON, we placed a microdialysis loop on the ventral surface of the SON, where the dendrites form a dense mat[12]. We applied electrical stimuli to the neural stalk to evoke antidromically propagated action potentials in supraoptic neurons. Stimulation produced a large release of oxytocin from the SON in thapsigargin-pretreated rats (Fig. 1c), but not in control rats, despite causing a large secretion of oxytocin into the plasma (data not shown). Thus exposure to thapsigargin appears to 'prime' activity-dependent oxytocin release from dendrites.

To test whether this priming action was specific to dendrites, we studied oxytocin release from isolated neural lobes and SON *in vitro*. Oxytocin secretion from the neural lobe, evoked by depolarization with high K^+ solutions, was unaffected by thapsigargin, caffeine and ryanodine, all of which can release Ca^{2+} from intracellular stores[11,13] (data not shown). By contrast, thapsigargin caused significant oxytocin release from the SON (Fig. 2a–d), whereas neither caffeine nor ryanodine had any appreciable effect on dendritic release (Fig. 2e–g). Furthermore, thapsigargin (but not caffeine or ryanodine) produced a marked potentiation of subsequent K^+-induced release ($P < 0.01$, paired *t*-tests; Fig. 2b–d). No potentiation was seen in response to high K^+ administered 5 min after exposure to thapsigargin (Fig. 2a), but large potentiation was observed in response to high K^+ administered 30, 60 or 90 min after thapsigargin (Fig. 2b–d). Application of an oxytocin agonist also induced significant oxytocin release from the SON ($P < 0.01$, paired *t*-tests), as shown previously[14], and, like thapsigargin, potentiated subsequent depolarization-evoked oxytocin release (Fig. 2h).

To investigate the physiological significance of priming of activity-dependent dendritic release, we recorded from single oxytocin neurons in virgin female rats while dialysing the SON with thapsigargin. Thapsigargin had no effect on the mean electrical discharge rate of cells (mean change in firing rate after 30 min exposure, -0.4 ± 0.4 spikes s^{-1}, $n = 7$), but statistical analysis revealed a subtle but important effect on discharge patterning. In oxytocin cells under control conditions, interspike intervals that are much shorter than the average interval tend to be followed by interspike intervals that are longer than average, reflecting the summating effects of slow post-spike hyperpolarization[15]. However, in some cells after thapsigargin treatment, intervals much shorter than average were followed by intervals that were also significantly shorter than average. This suggested that the normal post-spike hyperpolarization may be being over-ridden by post-spike depolarization, and hence that activity-dependent exocytosis from the dendrites may have a positive feedback effect on electrical activity.

If oxytocin (and/or other substances) released from dendrites affect the activity of neighbouring cells, then this should be particularly apparent from the effects of 'constant collision' stimulation (CCS, Fig. 3a)[16]. This protocol involves activating the neighbours of a recorded cell synchronously in an activity-dependent manner, mimicking the co-ordination of neuronal activity that precedes reflex milk ejection[17]. Electrical stimulus pulses applied to the neural stalk evoke antidromic spikes in all supraoptic neurons, except when a spike has occurred in the 10 ms before stimulation, in which case the antidromic spike evoked in that cell will be extinguished by collision with the descending spontaneous spike. During recording of each cell, stimuli (CCS) were applied to the neural stalk 5 ms after every spontaneous spike. Thus the CCS does not affect the

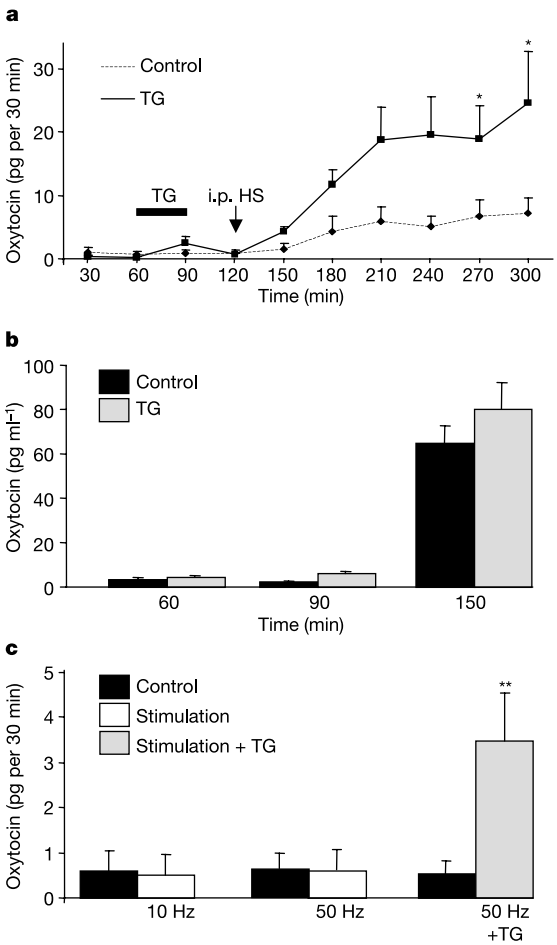

Figure 1 Oxytocin release in the SON. **a**, Release after intraperitoneal (i.p.) injection of hypertonic saline (HS) after dialysis of the SON with thapsigargin (TG) or control solution ($n = 6$). Asterisk, $P < 0.05$, analysis of variance (ANOVA). **b**, Oxytocin measured in the plasma in the same experiments as **a**. **c**, Oxytocin release in the SON before (filled bars) and after electrical stimulation of the neural stalk in control conditions and after exposure of the SON (unilaterally) to thapsigargin ($n = 8$). Double asterisk, $P < 0.01$, *t*-tests.

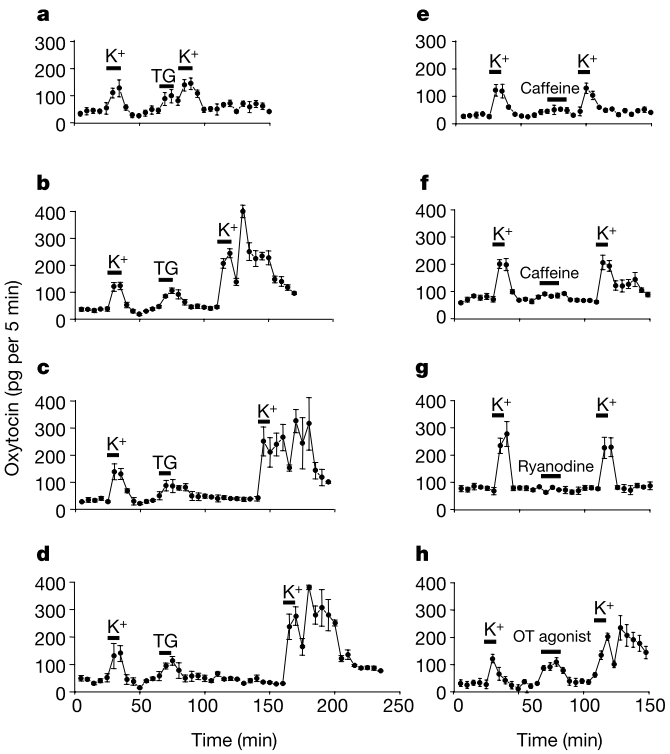

Figure 2 Effects of intracellular calcium mobilizers (horizontal bars) on oxytocin release *in vitro*. **a**–**g**, Secretion from isolated SON evoked by depolarization with high K^+ solutions was strongly potentiated by thapsigargin in a long lasting, time-dependent manner (**a**–**d**); by contrast, caffeine (**e**, **f**) and ryanodine (**g**) had negligible effects. **h**, Oxytocin release from the SON was also potentiated by exposure to an oxytocin (OT) agonist. Means ± standard error are shown; $n = 4$ per group for each experiment.

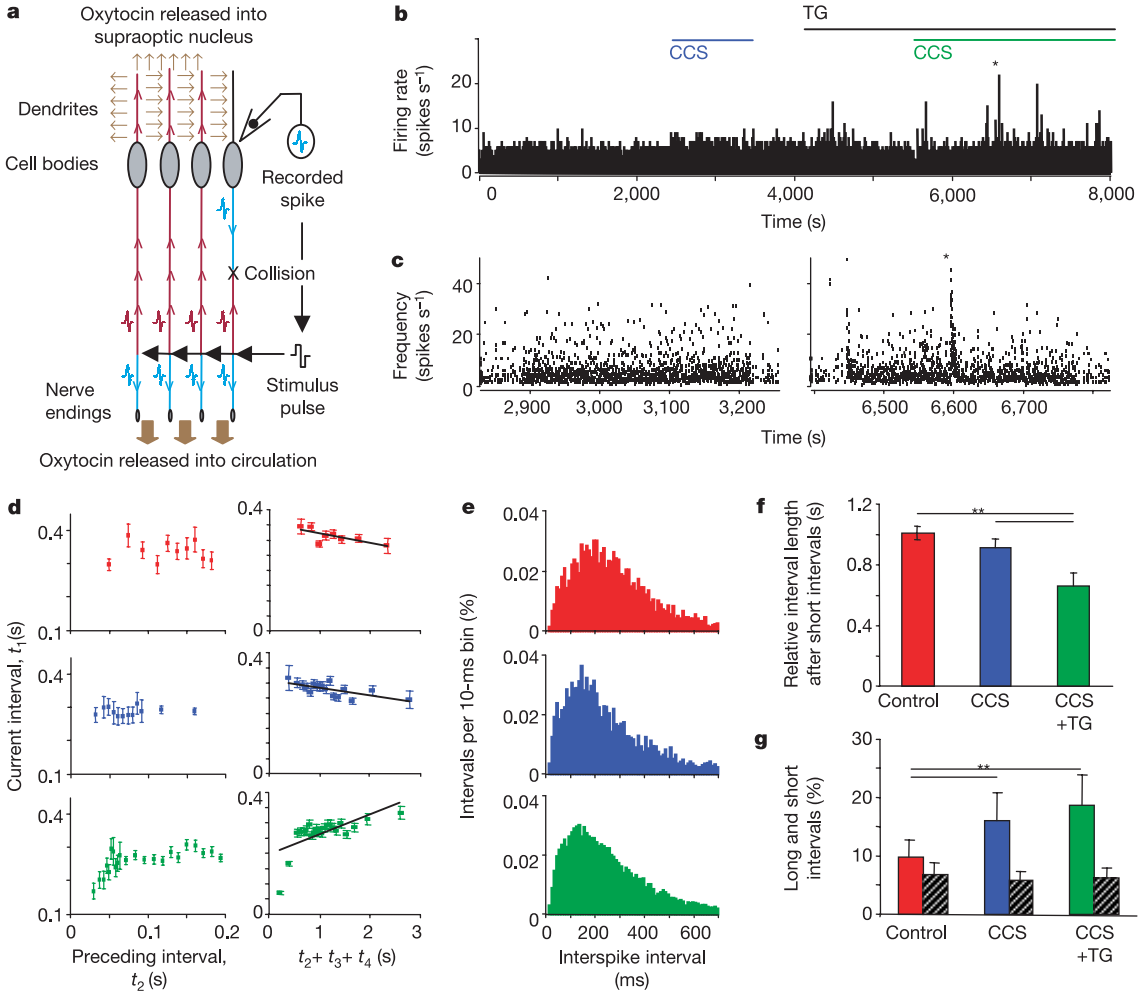

Figure 3 The effects of CCS (**a**) on a representative oxytocin cell (**b**–**e**), and data from 11 cells exposed to CCS after thapsigargin (**f**, **g**). After thapsigargin (administered by retrodialysis to the SON), CCS produced clustering of activity with occasional bursts (asterisks in **b**, **c**). **b**–**d**, Second-by-second firing rate (**b**), instantaneous frequency (**c**), and mean t_1 (± standard error) against t_2 and $t_2 + t_3 + t_4$, (with linear trend lines) for this cell in control conditions (red), during CCS (blue), and during CCS after thapsigargin treatment (green) (**d**) are shown. **e**, Corresponding interspike interval distributions. **f**, **g**, Data from 11 cells exposed to CCS after thapsigargin (means + standard error). Panel **f** shows the mean t_2 when following short values of t_1, compared to the overall mean t_2 for each cell. The bars show this ratio in control conditions (red), during CCS (blue), and during CCS after thapsigargin (green). **g**, Mean relative incidence of short intervals (less than 50 ms, hatched bars) and long intervals (greater than 700 ms, coloured bars) in the interspike interval distributions recorded in control conditions, during CCS and during CCS after thapsigargin. Double asterisk, $P < 0.01$, paired *t*-tests.

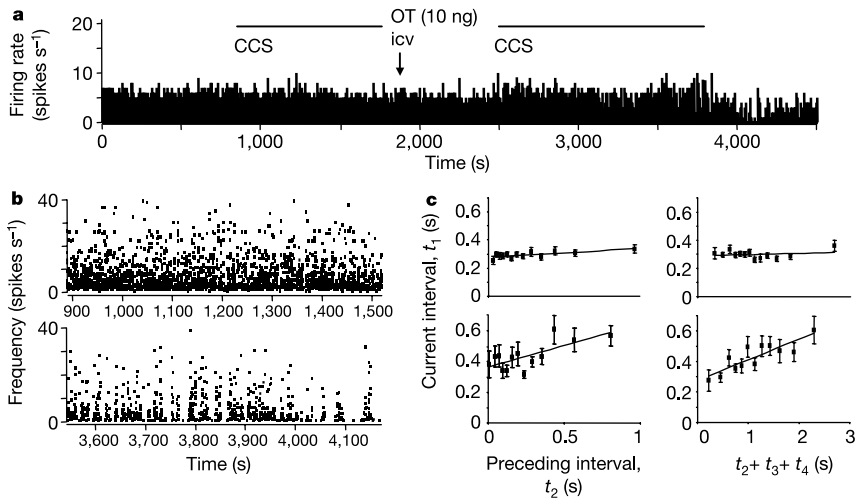

Figure 4 The effects of CCS on a representative oxytocin cell. After oxytocin microinjection (10 ng i.c.v.), CCS produced clustering of activity with occasional bursts. **a**–**c**, Second-by-second firing rate (**a**), instantaneous frequency (**b**) and mean t_1 (± standard error) against t_2, and $t_2 + t_3 + t_4$ (with linear trend lines) for this cell during CCS before (top panels) and after oxytocin injection (bottom panels) (**c**) are shown.

recorded cell directly, as all spikes evoked antidromically in that cell are extinguished; however, antidromic spikes cause approximately synchronous activation of neighbouring cells, and hence will cause synchronized activity-dependent exocytosis from neighbouring dendrites. CCS induces clustered discharge in some oxytocin cells with little effect on the mean discharge rate[16]. We compared current and preceding interspike intervals to look specifically for positive feedback effects. During CCS, 7 out of 11 cells showed a positive correlation between the current interspike interval and preceding interval lengths for the shortest intervals (Fig. 3). After thapsigargin treatment, positive correlations were stronger in each of the seven cells during CCS, and positive correlations were seen in the four cells that had not displayed them before thapsigargin treatment (Fig. 3d).

Overall, there was no change in the relative incidence of short intervals (less than 50 ms) in the cells tested with CCS. On the contrary, there was an increase in the incidence of long interspike intervals (greater than 700 ms) (Fig. 3g). Thus, during CCS after thapsigargin treatment, there is no increase in the firing rate of oxytocin cells, and no generally increased incidence of short intervals, but there is a re-organization of spike activity reflected by changes in the interspike interval distributions (Fig. 3e). Very short intervals tend to be followed by short intervals (Fig. 3f) in clusters of spikes that are followed by long intervals, and hence the second-by-second firing rate shows greater variability, as observed before suckling-induced bursts of milk ejection[17]. Some cells displayed clear bursts of activity[18] (Fig. 3b, c). These bursts were less intense than 'classical' milk-ejection bursts, which are characterized by extremely short interspike intervals (less than 10 ms) never normally seen in spontaneous activity[19], but were similar to bursts seen at the beginnings of reflex milk ejection[20].

In lactating rats, microinjections of oxytocin intracerebroventricularly (i.c.v.) or directly into the SON facilitate the suckling-induced milk ejection reflex for about 30 min[9]. In four experiments we applied CCS to oxytocin cells before and after i.c.v. injection of 10 ng oxytocin into the lateral ventricle. For three of the four cells tested, the effects of oxytocin on spike patterning during CCS were similar to those observed with thapsigargin (Fig. 4); the fourth cell tested was unaffected by oxytocin.

Thus mobilization of Ca^{2+} from thapsigargin-sensitive stores can evoke release of oxytocin from dendrites without an increase of electrical discharge rate and without triggering secretion from axon terminals. This may be a general neuronal mechanism: dendritic secretion of peptides and neurotransmitters has been described for many systems[2–4,21], and activity-dependent release of nerve growth factor from hippocampal neurons[22] is directly modulated by Ca^{2+} released from intracellular stores. Oxytocin itself mobilizes Ca^{2+} from thapsigargin-sensitive stores in oxytocin cells[11], and so, once triggered, oxytocin release may be self-sustaining and hence long lasting.

In addition, we show here that mobilization of intracellular Ca^{2+} is followed by a long-lasting potentiation (priming) of activity- or depolarization-dependent dendritic release. In oxytocin cells, thapsigargin produces a large rise in intracellular Ca^{2+} concentration ($[Ca^{2+}]_i$), but this effect is transient; $[Ca^{2+}]_i$ is elevated for only 5–10 min[11]. Hence the priming is not a consequence of long-lasting elevation of $[Ca^{2+}]_i$. Furthermore, the effect of thapsigargin is irreversible—the intracellular Ca^{2+} pools depleted by thapsigargin do not refill[23], thus priming cannot reflect a potentiation of intracellular Ca^{2+} release. Priming does not follow an increase in $[Ca^{2+}]_i$ *per se*, as no priming is induced by exposure to high K^+ alone. The depolarization-evoked rise in $[Ca^{2+}]_i$ is similar in magnitude to that following thapsigargin treatment[11], although it arises from Ca^{2+} entry through voltage-gated channels rather than from intracellular stores. It seems likely that Ca^{2+} release from intracellular stores recruits dendritic granules into a 'readily releasable pool', where they remain available for activity-dependent release for a prolonged period.

After priming, activity-dependent dendritic release facilitates 'clustered' discharge patterning in oxytocin cells. Whether this is a direct action on oxytocin cells, or involves modulation of presynaptic neurotransmitter release[24] or actions on interneurons[25], is not determined. However, it seems probable that this mechanism underlies the oxytocin-dependent generation of bursting activity in response to suckling. □

Methods

Microdialysis

Adult female rats were anaesthetized with ethyl carbamate (1.25 g kg^{-1} intraperitoneally). The pituitary stalk and SON were exposed transpharyngeally[26]. A U-shaped dialysis probe was positioned with the loop of the membrane flat on the ventral surface of the SON[12]. Oxytocin was measured by radio-immunoassay in fractions of microdialysate collected every 30 min[7]. In stimulation experiments, an electrode placed on the neural stalk[16] delivered phasic (1 mA, 2-ms matched biphasic pulses; 50 Hz for 3 s/10 s) or continuous stimulation (10 Hz) for 30 min. Blood samples were taken for measurement of oxytocin 5 min before and at the end of stimulation.

Oxytocin release from SON and neural lobes

Female rats (100–200 g) were decapitated, and the SON and neural lobe incubated in oxygenated Locke buffer (four SON or one lobe per well). Drugs (50 mM K^+, 200 nM thapsigargin, 20 mM caffeine, 2 μM ryanodine, 1 μM oxytocin agonist [Thr4,Gly7]oxytocin; Sigma) were applied for 10–15 min. Oxytocin was measured in 5-min samples of the incubate[27].

Electrophysiology

In anaesthetized rats, the activity of antidromically identified SON neurons was recorded, and vasopressin neurons and oxytocin neurons were distinguished by functional and electrophysiological criteria[12]. Artificial cerebrospinal fluid (ACSF) was dialysed at 3 μl min^{-1}. During recording, dialysis fluid was changed to ACSF containing thapsigargin (0.2 mM, Sigma). Cells were tested with CCS[16] before and after exposure to thapsigargin (applied by retrodialysis) or oxytocin (applied i.c.v.). Interspike interval histograms were constructed in each condition, and scaled to the total number of intervals recorded. Spike trains were analysed for serial dependence. In each period analysed, every interval t_1 was paired with its predecessor t_2 and the preceding trains ($t_2 + t_3 \ldots t_n$). The arrays were sorted by ascending t_1, and binned (bin size 50 for the shortest values of t_1; bin size 250 thereafter). For each bin, the corresponding means (+ standard error) of t_2 and ($t_2 + t_3 \ldots t_n$) were calculated.

Received 15 March; accepted 15 April 2002; doi:10.1038/nature00822.

1. Hausser, M., Stuart, G., Racca, C. & Sakmann, B. Axonal initiation and active dendritic propagation of action potentials in substantia nigra neurons. *Neuron* **15,** 637–647 (1995).
2. Zilberter, Y., Kaiser, K. M. M. & Sakmann, B. Dendritic GABA release depresses excitatory transmission between layer 2/3 pyramidal and bitufted neurons in rat neocortex. *Neuron* **24,** 979–988 (1999).
3. Isaacson, J. S. & Strowbridge, B. W. Olfactory reciprocal sysnapses—dendritic signalling in the CNS. *Neuron* **20,** 749–761 (1998).
4. Isaacson, J. S. Mechanisms governing dendritic γ-aminobutyric acid (GABA) release in the rat olfactory bulb. *Proc. Natl Acad. Sci. USA* **98,** 337–342 (2001).
5. Pow, D. V. & Morris, J. F. Dendrites of hypothalamic magnocellular neurons release neurohypophysial peptides by exocytosis. *Neuroscience* **32,** 435–439 (1989).
6. Moos, F. *et al.* Release of oxytocin within the supraoptic nucleus during the milk ejection reflex in rats. *Exp. Brain Res.* **76,** 593–602 (1989).
7. Ludwig, M. Dendritic release of vasopressin and oxytocin. *J. Neuroendocrinol.* **10,** 881–896 (1998).
8. Lincoln, D. W. & Wakerley, J. B. Electrophysiological evidence for the activation of supraoptic neurones during the release of oxytocin. *J. Physiol.* **242,** 533–554 (1974).
9. Lambert, R. C., Moos, F. C. & Richard, P. Action of endogenous oxytocin within the paraventricular or supraoptic nuclei: a powerful link in the regulation of the bursting pattern of oxytocin neurons during the milk-ejection reflex in rats. *Neuroscience* **57,** 1027–1038 (1993).
10. Leng, G., Brown, C. H. & Russell, J. A. Physiological pathways regulating the activity of magnocellular neurosecretory cells. *Prog. Neurobiol.* **57,** 625–655 (1999).
11. Lambert, R. C., Dayanithi, G., Moos, F. C. & Richard, P. A rise in the intracellular Ca^{2+} concentration of isolated rat supraoptic cells in response to oxytocin. *J. Physiol.* **478,** 275–288 (1994).
12. Ludwig, M. & Leng, G. Autoinhibition of supraoptic nucleus vasopressin neurons *in vivo*—a combined retrodialysis/electrophysiological study in rats. *Eur. J. Neurosci.* **9,** 2532–2540 (1997).
13. Berridge, M. J., Bootman, M. D. & Lipp, P. Calcium—a life and death signal. *Nature* **395,** 645–648 (1998).
14. Moos, F. *et al.* Release of oxytocin and vasopressin by magnocellular nuclei *in vitro*: specific facilitatory effect of oxytocin on its own release. *J. Endocrinol.* **102,** 63–72 (1984).
15. Kirkpatrick, K. & Bourque, C. W. Activity dependence and functional role of the apamin-sensitive K^+ current in the rat supraoptic neurones *in vitro*. *J. Physiol.* **494,** 389–398 (1996).
16. Leng, G. The effects of neural stalk stimulation upon firing patterns in rat supraoptic neurones. *Exp. Brain Res.* **41,** 135–145 (1981).
17. Brown, D. & Moos, F. Onset of bursting in oxytocin cells in suckled rats. *J. Physiol.* **503,** 625–634 (1997).
18. Lincoln, D. W. & Wakerley, J. B. Accelerated discharge of paraventricular neurosecretory cells correlated with reflex release of oxytocin during suckling. *J. Physiol.* **111,** 327–327 (1972).
19. Dyball, R. E. & Leng, G. Regulation of the milk ejection reflex in the rat. *J. Physiol.* **380,** 239–256 (1986).
20. Belin, V. & Moos, F. Paired recordings from supraoptic and paraventricular oxytocin cells in suckled rats: recruitment and synchronization. *J. Physiol.* **377,** 369–390 (1986).
21. Cheramy, A., Leviel, V. & Glowinski, J. Dendritic release of dopamine in the substantia nigra. *Nature* **289,** 537–542 (1981).
22. Blöchl, A. & Thoenen, H. Localization of cellular-storage compartments and sites of constitutive and

activity-dependent release of nerve growth factor in primary cultures of hippocampal neurons. *Mol. Cell. Neurosci.* **7,** 173–190 (1996).
23. Treiman, M., Caspersen, C. & Christensen, S. B. A tool coming to age: thapsigargin as an inhibitor of sarco-endoplasmic reticulum Ca^{2+}-ATPases. *Trends Pharmacol. Sci.* **19,** 131–135 (1998).
24. Kombian, S. B., Mouginot, D. & Pittman, Q. J. Dendritic released peptides act as retrograde modulators of afferent excitation in the supraoptic nucleus *in vitro*. *Neuron* **19,** 903–912 (1997).
25. Jourdain, P. *et al.* Evidence for a hypothalamic oxytocin-sensitive pattern-generating network governing oxytocin neurons *in vitro*. *J. Neurosci.* **18,** 6641–6649 (1998).
26. Leng, G. & Dyball, R. E. J. in *Neuroendocrine Research Methods* (ed. Greenstein, B.) 769–791 (Harwood GmbH, Switzerland, 1991).
27. Chevaleyre, V., Dayanithi, G., Moos, F. C. & Desarmenien, M. G. Developmental regulation of a local positive autocontrol of supraoptic neurons. *J. Neurosci.* **20,** 5813–5819 (2000).

Acknowledgements

The work was supported by the European Union, the Wellcome Trust, the DAAD/ARC, the British Council and the Alliance Franco-British Partnership Programme.

Competing interests statement

The authors declare that they have no competing financial interests.

Correspondence and requests for materials should be addressed to M.L. (e-mail: mike.ludwig@ed.ac.uk).

Capacitance steps and fusion pores of small and large-dense-core vesicles in nerve terminals

Vitaly A. Klyachko & Meyer B. Jackson

Department of Physiology and Biophysics Graduate Program, University of Wisconsin-Madison, 1300 University Avenue, Madison, Wisconsin 53706, USA

The vesicles that package neurotransmitters fall into two distinct classes, large dense-core vesicles (LDCVs) and small synaptic vesicles, the coexistence of which is widespread in nerve terminals[1]. High resolution capacitance recording reveals unitary steps proportional to vesicle size. Measurements of capacitance steps during LDCV and secretory granule fusion in endocrine and immune cells have provided important insights into exocytosis[2–4]; however, extending these measurements to small synaptic vesicles has proven difficult. Here we report single vesicle capacitance steps in posterior pituitary nerve terminals. These nerve terminals contain neuropeptide-laden LDCVs, as well as microvesicles. Microvesicles are similar to synaptic vesicles in size, morphology[5] and molecular composition[6–8], but their contents are unknown. Capacitance steps of two characteristic sizes, corresponding with microvesicles and LDCVs, were detected in patches of nerve terminal membrane. Both types of vesicles fuse in response to depolarization-induced Ca^{2+} entry. Both undergo a reversible fusion process commonly referred to as 'kiss-and-run', but only rarely. Fusion pores seen during microvesicle kiss-and-run have a conductance of 19 pS, 11 times smaller than LDCV fusion pores. Thus, LDCVs and microvesicles use structurally different intermediates during exocytosis.

An electron micrograph illustrates the two classes of vesicles described previously in the posterior pituitary[5] (Fig. 1a). To detect unitary capacitance steps during microvesicle and LDCV fusion, we improved the method of cell-attached capacitance measurement[9], reducing the noise level to less than 10 aF root mean square (r.m.s.) (where 1 aF is 10^{-18} farads). Figure 1b, c shows spontaneous upward and downward steps in capacitance, corresponding to the exo- and endocytosis, respectively, of single vesicles. The steps clearly fall into two size groups: the distribution of up-steps has two peaks, one centred at ~50 aF and the other at ~400 aF (Fig. 1d). The average amplitude in the range 20–120 aF was 67.0 ± 1.7 aF ($N = 235$, from more than 50 patches), and the average amplitude in the range 120–1,500 aF was 412 ± 16 aF ($N = 746$, from more than 50 patches). Assuming spherical geometry, and using a conversion factor of 0.9 μF cm^{-2} (ref. 10), we computed the vesicle diameter for each event and averaged these values to obtain 48.5 ± 0.7 nm ($N = 235$) for the small steps and 125 ± 1 nm ($N = 746$) for the large steps. This distribution is consistent with ultrastructural analysis of pituitary nerve terminals showing a mean diameter of 160 nm for LDCVs and ~50 nm for microvesicles (ref. 5). Thus, the two classes of capacitance steps observed here correspond well with the two classes of vesicles seen in nerve terminals (Fig. 1a). Essentially all patches of nerve terminal membrane showed some vesicle activity, with 65% of patches showing both LDCV and microvesicle steps, 25% showing LDCV steps only, and 10% showing microvesicle steps only.

We also examined downward capacitance steps. An amplitude distribution of down-steps not immediately preceded by an up-step (that is, not part of a kiss-and-run sequence, see below) showed that most down-steps were in the microvesicle size range (Fig. 1e). However, the distribution was broader, suggesting an endocytosis pathway into a population of vesicles similar but not identical to the vesicles that undergo exocytosis. Stimulation of the posterior pituitary induces labelling of microvesicles with extracellular markers[11], but leaves their overall number unchanged[12]. Thus, the endocytosis that rapidly follows exocytosis in this preparation[13] maintains a nearly constant total number of microvesicles. Large endocytosis steps (greater than 1.5 fF) that we attributed to endosome or vacuole trafficking[14] were also observed, but only rarely (five events).

Membrane depolarization increased the rate of fusion of both LDCVs and microvesicles (Fig. 2). The depolarization method used here—application of 115–130 mM KCl—collapses the K^+ gradient, and reduces the membrane potential from its resting value of −67 mV to about −20 mV (measured in current clamp). Experiments with the Ca^{2+}-sensitive fluorescent dye fluo-4 showed that this procedure increased intracellular Ca^{2+} concentration from 160 ± 30 nM to 500 ± 180 nM ($N = 5$). This depolarization increased the frequency of capacitance steps, producing an upward staircase (Fig. 2a). Depolarization had no effect in 55% of the patches tested. Some of these patches showed high activity before depolarization, suggesting elevated initial intracellular Ca^{2+}. In other recordings, the depth of the nerve terminal within the tissue may limit KCl access. In patches sensitive to KCl, the distribution of depolarization-induced up-steps included events in the size range for both microvesicles and LDCVs (Fig. 2b). In these patches, the increase in frequency was seen for both small (less than 120 aF) and large (greater than 120 aF) steps (Fig. 2c), indicating that both LDCVs and microvesicles undergo Ca^{2+}-triggered exocytosis. This exocytosis of LDCVs fits with their established role in neuropeptide release; however, Ca^{2+}-triggered exocytosis has not been demonstrated previously for posterior pituitary microvesicles, and the present result suggests that these vesicles have a functional capability similar to that of small synaptic vesicles.

For approximately 5% of the spontaneous up-steps, a down-step with the same amplitude followed within <2 s. These sequential up- and down-steps, referred to as capacitance flickers, had sizes consistent with both LDCVs (Fig. 3a) and microvesicles (Fig. 3b). Flickers were most readily recognized in the absence of depolarization. In depolarized patches the high level of activity made it difficult to associate a down-step unambiguously with a preceding up-step. Capacitance flickers are a common feature in LDCV exocytosis[2,3], and have been interpreted as the reversal of an early step in vesicle fusion[15]. They can thus be regarded as evidence for kiss-and-run exocytosis[16]. The apparent similarity between up- and down-steps was confirmed by analysing the correlation in amplitudes for LDCVs (Fig. 3c) and microvesicles (Fig. 3d). The amplitude of the down-step was tightly correlated with the amplitude of the paired up-step ($P < 0.0001$ for both). By contrast, down-steps